



This discussion paper is/has been under review for the journal Atmospheric Chemistry and Physics (ACP). Please refer to the corresponding final paper in ACP if available.

Further evidence of important environmental information content in red-to-green ratios as depicted in paintings by great masters

C. S. Zerefos^{1,2}, P. Tetsis¹, A. Kazantzidis³, V. Amiridis⁴, S. C. Zerefos⁵, J. Luterbacher⁶, K. Eleftheratos⁷, E. Gerasopoulos^{2,8}, S. Kazadzis⁸, and A. Papayannis⁹

¹Academy of Athens, Athens, Greece

²Navarino Environmental Observatory (N.E.O.), Messinia, Greece

³Laboratory of Atmospheric Physics, Physics Department, University of Patras, Greece

⁴Institute of Astronomy, Astrophysics, Space Application and Remote Sensing, National Observatory of Athens, Greece

⁵Hellenic Open University, Patras, Greece

⁶University of Giessen, Germany

⁷Faculty of Geology and Geoenvironment, University of Athens, Greece

⁸Institute of Environmental Research and Sustainable Development, National Observatory of Athens, Greece

Title Page

Abstract

Introduction

Conclusions

References

Tables

Figures

◀

▶

◀

▶

Back

Close

Full Screen / Esc

Printer-friendly Version

Interactive Discussion



⁹National Technical University of Athens, Athens, Greece

Received: 11 November 2013 – Accepted: 30 November 2013
– Published: 18 December 2013

Correspondence to: C. S. Zerefos (zerefos@geol.uoa.gr)

Published by Copernicus Publications on behalf of the European Geosciences Union.

ACPD

13, 33145–33176, 2013

**Atmospheric
aerosols and R/G
ratios in paintings**

C. S. Zerefos et al.

Title Page

Abstract

Introduction

Conclusions

References

Tables

Figures



Back

Close

Full Screen / Esc

Printer-friendly Version

Interactive Discussion



Abstract

This work is a follow-up study of a research carried out since 2005 and presents evidence supporting the findings of an earlier paper (Zerefos et al., 2007), which postulated that sunsets painted by famous artists provide independent proxy information on the aerosol optical depth after major volcanic eruptions. The series of these and additional paintings have been revisited and comparisons between coarser digital images with those derived from precision colour protocols, match together confirming the earlier results as discussed in the text. It was also found that aerosol optical depths (AODs) at 550 nm calculated by feeding Red-to-Green (R/G) ratios from a large number of paintings to a radiative transfer model, were well correlated with independent proxies from stratospheric AOD and optical extinction data, the dust veil index and others. AODs calculated from paintings have been grouped into 50 yr intervals from 1500 to 2000. From each 50 yr time period the year of the eruption and the 3 following years have been excluded. The remaining years have been termed “non-volcanic” and they provide additional evidence of a multidecadal increase in the atmospheric optical depths during the industrial “revolution”. The increase of AOD at 550 nm calculated from the paintings, is estimated to range from 0.15 in the middle 19th century to about 0.20 by the end of the 20th century. To corroborate our findings, an experiment was designed in which a master painter/colourist painted successive sunsets during and after the passage of Saharan aerosols over the island of Hydra in Greece. Independent solar radiometric measurements confirmed that the master colourist’s R/G ratios which were used to model his AODs, matched to the AOD values measured in situ by the co-located sunphotometers at the declining phase of the Sahara aerosol. Our work concludes that regardless of the school, red-to-green ratios from great masters can provide independent proxy AODs that correlate with widely accepted proxies and with independent measurements.

Atmospheric aerosols and R/G ratios in paintings

C. S. Zerefos et al.

Title Page

Abstract

Introduction

Conclusions

References

Tables

Figures

◀

▶

◀

▶

Back

Close

Full Screen / Esc

Printer-friendly Version

Interactive Discussion



1 Introduction

In the paper by Zerefos et al. (2007), the monochromatic ratios between red, green and blue colours, in paintings before, during and after large volcanic eruptions were examined. In that study, digital images from 554 paintings were downloaded from the websites of several art galleries and museums. These images were processed to derive ratios between the intensities of monochromatic colours. The study by Zerefos et al. (2007) concluded that regardless of the school or the style of the painter, the Red/Green (R/G) ratios at low solar elevation angles, correlated well to the modelled aerosol optical depth (AOD) values, following large volcanic eruptions. After its publication we were faced with the dilemma that the various digital images available at the above-mentioned websites were not necessarily accurate representations of the true colour profile reproduction, because they were not created following a single colour profile protocol and thus, we decided to revisit the issue.

In this work we provide new evidence that our earlier results, based on R/G ratios to estimate and model AODs in paintings are robust, a hypothesis which is supported using the following three methods: Firstly, by correlating the available R/G ratios from the above-mentioned public websites with the same ratios from their respective high quality colour profile protocols. Secondly, by comparing our earlier results of AODs based on art, with results and indices from other proxies (ice cores, pyrroliometric and other data) which cover the past 500 yr (Lamb, 1970, 1977, 1983; Robertson et al., 2001; Sato et al., 1993; Stothers, 1996, 2001). Thirdly, by performing an experiment involving the creation of sunset paintings and then measuring the ratios of the art piece with collocated AOD measurements actually recorded in the atmosphere during and after the passage of a Sahara-dust event. More specifically, we have organized an experimental campaign where Panayiotis Tetsis¹ (a well-known Greek landscape painter and colourist) painted the sunsets at the Hydra island in the Aegean Sea, during and after the passage of a Sahara dust event on the 19 and 20 June 2010. During the creation

¹<http://www.wikipaintings.org/en/panayiotis-tetsis>

Title Page

Abstract

Introduction

Conclusions

References

Tables

Figures

◀

▶

◀

▶

Back

Close

Full Screen / Esc

Printer-friendly Version

Interactive Discussion



direct or indirect measurements through clear shades, to facilitate the estimate of solar zenith angle, pertaining to each painting.

The high quality/resolution images obtained directly from the National Gallery, were next compared to their corresponding low quality/resolution images obtained from the website (<http://www.nationalgallery.org.uk/cgi-bin/WebObjects.dll/CollectionPublisher>), to test further the results obtained from the Tate Gallery comparisons shown in Figs. 1 and 2.

The retrieved R/G values of these images are shown in Fig. 3, from which we see that on the average, the R/G values are overestimated by 0.04 ± 0.08 . This result is in agreement with the results from the Tate Gallery sample of paintings and a tentative result is that the overestimation is larger (up to 0.3) deviating from the linear fit for the higher R/G values. At any rate, the correlation coefficients are still highly significant (99 % C.L.). It should be noted here that all images in this study were processed with the “nip2” software (e.g. <http://www.vips.ecs.soton.ac.uk/index.php?title=Nip2>) which comfortably works with multi-gigabyte images. A special work script has been created in order to calculate the average R/G values of the sky from each painting, as derived from the low and high quality/resolution images.

3 Other factors that might affect the R/G ratios from paintings

When trying to estimate a number that would describe the true colour at given solar zenith angle during a sunset, there are several factors that are important sources of uncertainty. Among them included are the coatings, the degradation of colour due to ageing, the unknown systematic practices used by the painters, the mood of the painter and the different styles of schools. However, we have to keep in mind that the earlier and present findings, of a relation between high aerosol content at sunsets, were *not based on true colours* but *confined only to the case of the R/G ratios*. The different factors affecting the true colours mentioned above, being either random or systematic, may also affect the R/G ratios. Although this may be true for an individual painting,

Atmospheric aerosols and R/G ratios in paintings

C. S. Zerefos et al.

Title Page

Abstract

Introduction

Conclusions

References

Tables

Figures

◀

▶

◀

▶

Back

Close

Full Screen / Esc

Printer-friendly Version

Interactive Discussion



the statistics presented here show that when a large number of paintings by different painters is considered, these uncertainties are much reduced or even cancelled out by the averaging process.

In our study, a detailed quantification of each source of uncertainty, apart from the low quality digitalization of the paintings, was not possible to be performed. Despite all these uncertainties, the use of the R/G ratios seems to provide valuable information, since as mentioned before and shown in the next paragraphs, high and significant correlations were found with volcanic indices based on completely independent techniques as well as proxies used by other scientists (see Sect. 4). The latter indicates that the signal included in the average ratios is possibly higher than any random or systematic errors in the noise level of the R/G time series.

4 Atmospheric optical depths based on known proxies and on R/G ratios of paintings in the past 500 yr

The earlier estimates of the aerosol optical depth at 550 nm (based on R/G calibrated ratios from paintings) and the radiative transfer model by Mayer and Kylling (2005) and Mayer and Emde (2007), were used to compile an independent time series with AODs during 1500–2000 AD. This long term data set of AODs is compared to other proxies as shown in Fig. 4. The reader is referred here to the articles describing these proxies, such as Lamb (1970, 1977, 1983), Robertson et al. (2001), Sato et al. (1993) and Stothers (1996, 2001). Using the data shown in Fig. 4 we show in Table 1, that the correlation coefficients between other proxy indices and the estimated AODs from the R/G ratios from paintings are statistically significant.

The reader is also referred to the precision by which the extreme AODs between paintings and proxies during large volcanic eruptions match in most cases. In particular, in 102 cases for which data of both DVI and this study are simultaneously available, DVI spikes are coinciding to AOD spikes from this study at a percentage of 80% (9 out of 11 cases). As spikes we define the values in both time series that belong in the

Atmospheric aerosols and R/G ratios in paintings

C. S. Zerefos et al.

Title Page

Abstract

Introduction

Conclusions

References

Tables

Figures



Back

Close

Full Screen / Esc

Printer-friendly Version

Interactive Discussion



upper 10% range of values. In addition, this study revealed two high AOD cases that do not match with DVI spikes and it is worth noting that both failing cases succeeded a period of two consecutive years with spikes in both indices.

We note here that using an independently calculated index of total sulphate at Greenland ice cores² (Zielinski, 1995; Zielinski et al., 1996) and the longer time series of stratospheric AOD (Robertson et al., 2001) when grouped in 50 yr time intervals, they correlate with the corresponding AODs calculated from the R/G ratios in the paintings. More analytically, the time series of AODs calculated from paintings has been divided into 50 yr intervals from 1500 to 2000. From each 50 yr time period the year of the eruption and the 3 following years have been excluded. The remaining years have been termed “non-volcanic” from which we have calculated the average AOD value pertaining to these years. The same procedure has been followed for the case of stratospheric AOD and total sulphate from ice core as seen in Fig. 5. We note here the point raised by Robertson et al. (2001) that the last 150 yr increase in total sulphate from ice core was hypothesized to be the result of tropospheric anthropogenic sulfate deposition. The point by Robertson et al. is worth emphasizing since there have been no major volcanic eruptions between 1900 and 1960. A list of major volcanic eruptions in the past 500 yr can be found in Table A2 (after Ammann and Naveau, 2003; Robock, 2000). It can be easily seen that compared to the pre-industrial period, the industrial period shows higher aerosol content, as it is well known and expected from the literature (e.g Neftel et al., 1985; Robock and Free, 1995; Robertson et al., 2001; IPCC, 2007).

²Total sulphate is the total measured sulphate concentration in ppb in the core, as resulted from deposition either from the stratosphere (volcanic) or the troposphere (anthropogenic and other biogenic sources), as described by Zielinski et al. (1996) and Robertson et al. (2001). The presented values do not refer directly to the atmospheric concentration, but rather to the deposition on ice which however is related to ambient concentrations.

Atmospheric aerosols and R/G ratios in paintings

C. S. Zerefos et al.

Title Page

Abstract Introduction

Conclusions References

Tables Figures

◀ ▶

◀ ▶

Back Close

Full Screen / Esc

Printer-friendly Version

Interactive Discussion



5 A live case: the Hydra experiment

To corroborate our findings, a dedicated experimental campaign has been organized and implemented in Greece, aiming to evaluate the R/G retrieval methodology against ground-truth measurements of the aerosol load in terms of AOD values. The well-known colourist and landscape painter Panayiotis Tetsis (<http://www.wikipaintings.org/en/panayiotis-tetsis>) kindly offered to paint in real-time a number of sunsets at the island of Hydra. As the great master was painting, a suite of ground-based aerosol measurements has been collected, mainly by means of sunphotometry equipment.

5.1 Experiment organization and instrumentation

The experiment was conducted in Hydra, the painter's home base. Hydra is an island located in the Aegean Sea (37.21° N, 23.28° E), 80 km south of Athens, and has a population of about 2000 inhabitants. The size of the island satisfies the main requirement for negligible local aerosol emissions (cars are not allowed in the island). Apart from sea spray particles, that constitute the background aerosol component around the island, the only case of regional pollution influence is under northerly winds when the island is within the outflow of pollution from Athens. In the case of winds from southerly directions, most of the Athenian sources of aerosols do not reach Hydra island.

For the design of the experiment, paintings and measurements during relatively low and high AOD cases was the main goal. According to Gerasopoulos et al. (2011), the typical background AOD for the area is 0.12–0.13 corresponding to long and fast trajectories from westerly to northerly directions, with origin from high altitudes over the Atlantic. Higher aerosol loading over the area is related to the advection of dust particles from desert and arid locations of North Africa and is in the AOD range of 0.3–0.4. The most frequent season for dust outbreaks over the Eastern Mediterranean is well documented to be in late spring (e.g. Kalivitis et al., 2007; Gerasopoulos et al., 2011) and early summer (the latter mostly as elevated dust layers; Papayannis et al., 2008).

**Atmospheric
aerosols and R/G
ratios in paintings**

C. S. Zerefos et al.

Title Page

Abstract

Introduction

Conclusions

References

Tables

Figures

◀

▶

◀

▶

Back

Close

Full Screen / Esc

Printer-friendly Version

Interactive Discussion



For the selection of the experiment days, a regional model designed to simulate and forecast the atmospheric cycle of mineral dust aerosol over the campaign site was deployed. In particular, forecasts from the BSC-DREAM8b dust regional model were used (Nickovic et al., 2001) and the period finally selected to combine an AOD episode followed by clean conditions and the painter's availability was 19–20 June 2010.

The instrumentation used for the needs of the campaign, included a Multi-Filter Rotating shadowband radiometer (MFR-7 Yankee Env. System Inc., Turner Falls, MA) and a Microtops II sunphotometer (Solar Light Inc., Philadelphia, USA). The MFR-7 installed at Hydra was used to perform measurements of the total and diffuse solar irradiance to calculate the direct component of the irradiance (Harrison et al., 1994). MFR-7 provided 1 min average measurements and from these the AOD values at 500 nm was extracted. The instrument performs valid measurements during daytime and under clear sky conditions. The methodology followed for the extraction of the AOD values from direct solar irradiance is thoroughly described in Gerasopoulos et al. (2003). The calibrated hand-held sunphotometer (Microtops II) was used to provide the AOD at 1020 nm, at 10 min intervals.

5.2 Results and discussion

As mentioned, the experiment took place in Hydra on 19 and 20 June 2010. During the campaign, a Saharan dust event passed over Greece (18–21 June 2010). On these two dates master Tetsis created two successive paintings; before and during sunset on the 19 and two additional paintings at sunset on the next day, the 20 June 2010. In the next paragraph it will be shown that the Saharan dust outbreak of the 19 June has been found to affect the R/G ratios of Tetsis' paintings.

The results from the BSC-DREAM8b model simulations of the space and time evolution of the columnar dust loading concentration (in gm^{-2}), for the campaign days (19 and 20 June) are shown in Fig. 6. Additionally, the wind fields at 3000 m heights are superimposed, showing clearly a Southwestern flow affecting the site in both campaign days. No precipitation or cloudiness prevailed over Greece during the campaign pe-

**Atmospheric
aerosols and R/G
ratios in paintings**

C. S. Zerefos et al.

Title Page

Abstract

Introduction

Conclusions

References

Tables

Figures

◀

▶

◀

▶

Back

Close

Full Screen / Esc

Printer-friendly Version

Interactive Discussion



riod (Fig. 6 – upper panel), also corroborated by MODIS satellite images (not shown here). A massive transport of dust from Sahara desert is observed on the 19 June over Greece and West Turkey, while on 20 June the centre of the dust plume spread and declined over the eastern parts of Greece (Fig. 6 – lower panel). Following the BSC-DREAM8b simulations, the dust load reached maximum columnar concentration values of the order of 0.75 gm^{-2} over the Hydra site on the 19 June.

The model simulations agree with real-time measurements, as shown in Fig. 7 by the time evolution of the observed AOD values on site for 19 and 20 June, measured with MFR-7 and Microtops. As stated before, the local pollution at Hydra is considered negligible and under southerly flows urban pollution from Athens does not reach the island. The meteorological conditions prevailing during both days (at sunset hours) were similar, namely temperatures between 28 and 30 °C (slightly higher on the second day) relative humidity between about 45 and 60 %, and calm wind conditions ($1\text{--}2 \text{ ms}^{-1}$). The AOD values observed at Hydra, to their largest part, can be attributed to the presence of the Saharan dust aerosol and follow the temporal evolution depicted by the dust simulations shown in Fig. 6, from which we see higher AOD values on 19 June and lower on the next day at Hydra. The temporal decay is profound also in the Microtops measurements at 1020 nm, performed at Hydra and shown also in Fig. 7.

Sunphotometric measurements are a trustworthy source for identifying the Saharan dust presence, for which we expect higher AOD values and lower spectral dependences between the multi-wavelength AOD retrievals. This is clearly seen in the data presented in Fig. 7, where higher AODs for 19 June are accompanied with lower spectral dependences between the 500 and 1020 nm channels. Moreover, the respective Ångström exponents were on average 0.4 on the first day, indicative of coarse dust aerosols and in the range 0.7–1.0 on the second day, representing a mixture of sea salt particles with low loadings of continental aerosols (see Gerasopoulos et al., 2011, for indicative ranges of Ångström exponents in the area).

Acknowledging the good performance of BSC-DREAM8b model for the days of our campaign, we present in Fig. 8 the simulations of the vertical distribution of Saharan

**Atmospheric
aerosols and R/G
ratios in paintings**

C. S. Zerefos et al.

Title Page

Abstract

Introduction

Conclusions

References

Tables

Figures

◀

▶

◀

▶

Back

Close

Full Screen / Esc

Printer-friendly Version

Interactive Discussion



dust concentrations over the area for 19 and 20 June 2010. As can be seen from that Figure, large dust concentrations in the lowest one kilometre were observed on the 19 June, while on the next day the dust concentrations declined significantly, in the boundary layer and in the column as well. We focus mainly on the aerosol load in the planetary boundary layer since this is expected to impact mostly the painter's perception during the late afternoon hours. It is evident that the dust concentrations within the first kilometre are four (4) times higher on 19 June than those simulated on 20 June.

Figure 9 shows the temporal evolution of the MFR-7 AOD values at 550 nm during the two days of the campaign together with the R/G ratios from a digital camera on site and from the high precision digital images (produced by National Gallery, London, with the methodology described in paragraph 2) of Tetsis paintings (Fig. 10) for the two sunset cases (high aerosol and low aerosol over Hydra). The paintings were transported to the National Gallery where the digital protocol analysis was done. On 19 June 2010 (Fig. 9, upper panel), the estimated AOD differences between the paintings and the closest time digital photos is ± 0.02 . However, a bias of about 30 % is revealed between these and the MFR measurements on the day of the Sahara dust event. In all three types of measurements/estimations, the variability of AOD with time shows a negative trend as we move from 19 June to the evening of 20 June. On 20 June 2010, the agreement between the digitally-derived and the measured AOD values is substantially improved: differences as small as 0.02 can be found. The measured decrease of the AOD values is also successfully represented by the digital estimations.

6 Conclusions

Understanding the atmospheric composition of the past centuries is a very difficult task due to scarcity of available measurements. Especially for atmospheric components such as aerosols and their variability over the past 500 yr, relevant information is rare (Thornes and Constable, 1999; Grattan, 2006; Zerefos et al., 2007). In this work we

**Atmospheric
aerosols and R/G
ratios in paintings**

C. S. Zerefos et al.

Title Page

Abstract

Introduction

Conclusions

References

Tables

Figures

◀

▶

◀

▶

Back

Close

Full Screen / Esc

Printer-friendly Version

Interactive Discussion



The master painter did not know anything about the passage of a Saharan dust event. Our independent sunphotometric measurements at Hydra confirmed that the calculated AOD values from R/G ratios measured in the master colourist paintings, matched quite well to the AOD values measured in situ as well as with measurements from a digital camera. It should be noted here that all four watercolours by Panayiotis Tetsis were digitized using the same procedures and standards applied to all works of art photographed by the Photographic Department of the National Gallery, London. These findings point to the conclusion that the experiment provides a new presentation of how a painter, a digital camera and scientific instruments capture changes in R/G ratios at high and low aerosol overhead cases.

Acknowledgements. The LibRadtran team (www.libradtran.org) is acknowledged for providing the model algorithm. The National Gallery is acknowledged for providing 186 landscape paintings of high quality analysis at no charge. BSC-DREAM8b Saharan dust simulations were kindly provided by the Barcelona Supercomputing Centre. The set of high resolution 124 paintings from Tate were purchased at cost and the four watercolour paintings by Panayiotis Tetsis were photographed using the same procedures and standards applied to all works of art photographed by the Photographic Department of the National Gallery, London. We greatly acknowledge the support provided by the Mariolopoulos-Kanaginis Foundation for the Environmental Sciences and the European Union's 7th Framework Programme (FP7/2007-2013) under Grant Agreement no. 218793 (project title: Monitoring Atmospheric Composition and Climate). The authors would like to thank the two anonymous reviewers for their valuable comments.

References

- Ammann, C. and Naveau, P.: Statistical analysis of tropical explosive volcanism occurrences over the last 6 centuries, *Geophys. Res. Lett.*, 30, 1210, doi:10.1029/2002GL016388, 2003.
- Gerasopoulos, E., Andreae, M. O., Zerefos, C. S., Andreae, T. W., Balis, D., Formenti, P., Merlet, P., Amiridis, V., and Papastefanou, C.: Climatological aspects of aerosol optical properties in Northern Greece, *Atmos. Chem. Phys.*, 3, 2025–2041, doi:10.5194/acp-3-2025-2003, 2003.

**Atmospheric
aerosols and R/G
ratios in paintings**

C. S. Zerefos et al.

Title Page

Abstract

Introduction

Conclusions

References

Tables

Figures

◀

▶

◀

▶

Back

Close

Full Screen / Esc

Printer-friendly Version

Interactive Discussion



- Gerasopoulos, E., Amiridis, V., Kazadzis, S., Kokkalis, P., Eleftheratos, K., Andreae, M. O., Andreae, T. W., El-Askary, H., and Zerefos, C. S.: Three-year ground based measurements of aerosol optical depth over the Eastern Mediterranean: the urban environment of Athens, *Atmos. Chem. Phys.*, 11, 2145–2159, doi:10.5194/acp-11-2145-2011, 2011.
- 5 Grattan, J.: Aspects of Armageddon: an exploration of the role of volcanic eruptions in human history and civilization, *Quartern. Int.*, 151, 10–18, 2006.
- Harrison, L., Michalsky, J., and Berndt, J.: Automated multifilter rotating shadow-band radiometer: an instrument for optical depth and radiation measurements, *Appl. Optics*, 33, 5118–5125, 1994.
- 10 IPCC: Climate Change 2007: The Physical Science Basis, Contribution of Working Group I to the Fourth Assessment, Report of the Intergovernmental Panel on Climate Change, edited by: Solomon, S., Qin, D., Manning, M., Chen, Z., Marquis, M., Averyt, K. B., Tignor, M., and Miller, H. L., Cambridge University Press, Cambridge, UK, New York, NY, USA, 996 pp., 2007.
- 15 Kalivitis, N., Gerasopoulos, E., Vrekoussis, M., Kouvarakis, G., Kubilay, N., Hatzianastassiou, N., Vardavas, I., and Mihalopoulos, N.: Dust transport over the Eastern Mediterranean from TOMS, AERONET and surface measurements, *J. Geophys. Res.*, 112, D03202, doi:10.1029/2006JD007510, 2007.
- Lamb, H. H.: Volcanic dust in the atmosphere, with a chronology and assessment of its meteorological significance, *Philos. T. R. Soc. Lon.*, 266, 425–533, 1970.
- 20 Lamb, H. H.: Supplementary volcanic dust veil assessments, *Climate Monitor*, 6, 57–67, 1977
- Lamb, H. H.: Uptake of the chronology of assessments of the volcanic dust veil index, *Climate Monitor*, 12, 79–90, 1983.
- Mayer, B. and Emde, C.: Comment on “Glory phenomenon informs of presence and phase state of liquid water in cold clouds” by Nevzorov, A. N., *Atmos. Res.*, 84, 410–419, 2007.
- 25 Mayer, B. and Kylling, A.: Technical note: The libRadtran software package for radiative transfer calculations – description and examples of use, *Atmos. Chem. Phys.*, 5, 1855–1877, doi:10.5194/acp-5-1855-2005, 2005.
- McCamy, C. S., Marcus, H., and Davidson, J. G.: A color-rendition chart, *J. Appl. Photogr. Eng.*, 2, 95–99, 1976.
- 30 Neffel, A., Beer, J., Oeschger, H., Zurcher, F., and Finkel, R. C.: Sulphate and nitrate concentrations in snow from South Greenland 1895–1978, *Nature*, 314, 611–613, doi:10.1038/314611a0, 1985.

Atmospheric aerosols and R/G ratios in paintings

C. S. Zerefos et al.

Title Page

Abstract

Introduction

Conclusions

References

Tables

Figures

◀

▶

◀

▶

Back

Close

Full Screen / Esc

Printer-friendly Version

Interactive Discussion



- Nickovic, S., Kallos, G., and Papadopoulos, A., Kakaliagou, O.: A model for prediction of desert dust cycle in the atmosphere, *J. Geophys. Res.*, 106, 18113–18129, doi:10.1029/2000JD900794, 2001.
- Papayannis, A., Amiridis, V., Mona, L., Tsaknakis, G., Balis, D., Bösenberg, J., Chaikovski, A., De Tomasi, F., Grigorov, I., Mattis, I., Mitev, V., Müller, D., Nickovic, S., Perez, C., Pietruczuk, A., Pisani, G., Ravetta, F., Rizi, V., Sicard, M., Trickl, T., Wiegner, M., Gerding, M., Mamouri, R. E., D'Amico, G., and Pappalardo, G.: Systematic lidar observations of Saharan dust over Europe in the frame of EARLINET (2000–2002), *J. Geophys. Res.*, 113, D10204, doi:10.1029/2007JD009028, 2008.
- Robertson, A., Overpeck, J., Rind, D., Mosley-Thompson, E., Zielinski, G., Lean, J., Koch, D., Penner, J., Tegen, I., and Healy, R.: Hypothesized climate forcing time series for the last 500 years, *J. Geophys. Res.*, 106, 14783–14803, 2001.
- Robock, A.: Volcanic eruptions and climate, *Rev. Geophys.*, 38, 191–219, 2000.
- Robock, A. and Free, M. P.: Ice cores as an index of global volcanism from 1850 to the present, *J. Geophys. Res.*, 100, 11549–11567, 1995.
- Sato, M., Hansen, J. E., McCormick, M. P., and Pollack, J. B.: Stratospheric aerosol optical depths 1850–1990, *J. Geophys. Res.*, 98, 22987–22994, 1993.
- Saunders, D., Cupitt, J., White, C., and Holt, S.: The MARC II camera and the scanning initiative at the national gallery, *National Gallery Technical Bulletin*, 23, 76–82, 2002.
- Stothers, R. B.: Major optical depth perturbations to the stratosphere from volcanic eruptions: pyrheliometric period 1881–1960, *J. Geophys. Res.*, 101, 3901–3920, 1996.
- Stothers, R. B.: Major optical depth perturbations to the stratosphere from volcanic eruptions: Stellar extinction period 1961–1978, *J. Geophys. Res.*, 106, 2993–3003, 2001.
- Thornes, J. E. and Constable, J.: *John Constable's skies: A Fusion of Art and Science*, Ed. Continuum, 288 p., ISBN-13: 978-1902459028, 1999.
- Zerefos, C. S., Gerogiannis, V. T., Balis, D., Zerefos, S. C., and Kazantzidis, A.: Atmospheric effects of volcanic eruptions as seen by famous artists and depicted in their paintings, *Atmos. Chem. Phys.*, 7, 4027–4042, doi:10.5194/acp-7-4027-2007, 2007.
- Zielinski, G. A.: Stratospheric loading and optical depth estimates of explosive volcanism over the last 2100 years derived from the Greenland Ice Sheet Project 2 ice core, *J. Geophys. Res.*, 100, 20937–20955, 1995.

Zielinski, G. A., Mayewski, P. A., Meeker, L. D., Whitlow, S., and Twickler, M. S.: A 110,000-yr record of explosive volcanism from the GISP2 (Greenland) ice core, *Quaternary Res.*, 45, 109–188, 1996.

Atmospheric aerosols and R/G ratios in paintings

C. S. Zerefos et al.

Title Page

Abstract

Introduction

Conclusions

References

Tables

Figures



Back

Close

Full Screen / Esc

Printer-friendly Version

Interactive Discussion



Atmospheric aerosols and R/G ratios in paintings

C. S. Zerefos et al.

Title Page

Abstract

Introduction

Conclusions

References

Tables

Figures

⏪

⏩

◀

▶

Back

Close

Full Screen / Esc

Printer-friendly Version

Interactive Discussion



Table 1. Correlation coefficients between volcanic aerosol indices and AOD proxies shown in Fig. 4.

1500–2000	DVI	AOD (this study)	AOD (Robertson)	AOD (Sato)	AOD (Stothers)
DVI	1				
AOD (this study)	0.85	1			
AOD (Robertson)	0.65	0.57	1		
AOD (Sato)	0.67	0.58	0.56	1	
AOD (Stothers)	(0.76)	0.62	(0.81)	(0.92)	1

Bold: confidence level 99 % (*t* test).
 In parentheses: based on less than 40yr of data.

Table A1. Paintings from the Tate Gallery analysed in this work.

Image ID	Artist Name	Title
1. D00670	Turner, Joseph Mallord William	Windmill on Hill: Valley and Winding River in Middle Distance; Sunset Effect
2. D02474	Turner, Joseph Mallord William	Helmsley Sketchbook [Finberg LIII], Distant View of Whitby from the Moors: A Windmill against a
3. D04118	Turner, Joseph Mallord William	Studies for Pictures Sketchbook [Finberg LXIX], Study for the Composition of "Dolbadern Castle"
4. D04119	Turner, Joseph Mallord William	Studies for Pictures Sketchbook [Finberg LXIX], Study for the Composition of "Dolbadern Castle"
5. D04127	Turner, Joseph Mallord William	Studies for Pictures Sketchbook [Finberg LXIX], Snowy Hills beside a Lake: ?Evening Sky
6. D04128	Turner, Joseph Mallord William	Studies for Pictures Sketchbook [Finberg LXIX], Study for the Composition of "Dolbadern Castle"
7. D08176	Turner, Joseph Mallord William	Moonlight at Sea (The Needles)
8. D12502	Turner, Joseph Mallord William	Skies Sketchbook [Finberg CLVIII], Red Sky and Crescent Moon
9. D16131	Turner, Joseph Mallord William	Naples: Rome. C. Studies Sketchbook [Finberg CLXXXVII], The Roman Campagna from Monte Testaccio
10. D16482	Turner, Joseph Mallord William	Small Roman Colour Studies Sketchbook [Finberg CXC], Moonlight over the Campagna
11. D20254	Turner, Joseph Mallord William	Mayen in the Eifel
12. D22663	Turner, Joseph Mallord William	Evening: A Windmill at Sunset
13. D22664	Turner, Joseph Mallord William	Sunset across the Park from the Terrace of Petworth House
14. D22666	Turner, Joseph Mallord William	Evening: A Boat on a River with a Distant Tower
15. D22674	Turner, Joseph Mallord William	Sunset over the Ridge Seen from the North Pond in Petworth Park
16. D22716	Turner, Joseph Mallord William	Setting Sun
17. D22719	Turner, Joseph Mallord William	The Setting Sun over Petworth Park
18. D22767	Turner, Joseph Mallord William	Petworth Park; Sunset ("Glade and Greensward")
19. D22768	Turner, Joseph Mallord William	Sunset: A Boat on a River
20. D24635	Turner, Joseph Mallord William	A Distant View of the Upperton Monument, from the Lake in Petworth Park
21. D24640	Turner, Joseph Mallord William	Harbour Scene at Sunrise, possibly Margate
22. D24666	Turner, Joseph Mallord William	The Scarlet Sunset
23. D24698	Turner, Joseph Mallord William	Turner's Annual Tour: The Seine 1834 Watercolours, Le Havre: Sunset in the Port
24. D24757	Turner, Joseph Mallord William	A View of Metz from the North
25. D25132	Turner, Joseph Mallord William	Sunlight over Water
26. D25141	Turner, Joseph Mallord William	Cilgerran Castle, Pembrokeshire
27. D25144	Turner, Joseph Mallord William	The River; Sunset
28. D25201	Turner, Joseph Mallord William	Looking out to Sea
29. D25233	Turner, Joseph Mallord William	River with Trees: Sunset
30. D25246	Turner, Joseph Mallord William	Castle Upnor, Kent: Preparatory Study
31. D25249	Turner, Joseph Mallord William	River: Sunset
32. D25253	Turner, Joseph Mallord William	Studies of Skies
33. D25258	Turner, Joseph Mallord William	Evening
34. D25263	Turner, Joseph Mallord William	The Line of Cliffs
35. D25300	Turner, Joseph Mallord William	The Castle by the Sea
36. D25303	Turner, Joseph Mallord William	River Scene: Sunset
37. D25315	Turner, Joseph Mallord William	Sunset
38. D25329	Turner, Joseph Mallord William	Sunset
39. D25330	Turner, Joseph Mallord William	Fiery Sunset
40. D25331	Turner, Joseph Mallord William	Crimson Sunset
41. D25332	Turner, Joseph Mallord William	Sunset over Water
42. D25336	Turner, Joseph Mallord William	A Ruin: Sunset
43. D25338	Turner, Joseph Mallord William	Twilight over the Waters
44. D25361	Turner, Joseph Mallord William	A Stormy Sunset
45. D25368	Turner, Joseph Mallord William	Sequels to the Liber Studiorum ("Little Liber") Watercolours, The Distant Tower: Evening
46. D25403	Turner, Joseph Mallord William	The Yellow Sky
47. D25412	Turner, Joseph Mallord William	A Pink Sky above a Grey Sea
48. D25430	Turner, Joseph Mallord William	Sequels to the Liber Studiorum ("Little Liber") Watercolours, Gloucester Cathedral
49. D25433	Turner, Joseph Mallord William	Running Wave in a Cross-Tide: Evening

Title Page

Abstract

Introduction

Conclusions

References

Tables

Figures



Back

Close

Full Screen / Esc

Printer-friendly Version

Interactive Discussion



Table A1. Continued.

Image ID	Artist Name	Title
50. D25443	Turner, Joseph Mallord William	Barnstaple Bridge at Sunset
51. D25446	Turner, Joseph Mallord William	Study for 'The Golden Bough
52. D25450	Turner, Joseph Mallord William	Sunset
53. D25474	Turner, Joseph Mallord William	Rochester Castle and Bridge
54. D25507	Turner, Joseph Mallord William	Sunset over the Sea
55. D25514	Turner, Joseph Mallord William	St Michael's Mount from Marazion, Cornwall
56. D27601	Turner, Joseph Mallord William	Sunset over a City
57. D27689	Turner, Joseph Mallord William	Rogers's Poems 1835 Watercolours, Tornaro (Rogers's "Poems")
58. D27716	Turner, Joseph Mallord William	Rogers's Poems 1835 Watercolours, Datur Hora Quieti
59. D28994	Turner, Joseph Mallord William	Sunset over Lake or River
60. D29026	Turner, Joseph Mallord William	Sunset
61. D32130	Turner, Joseph Mallord William	Roll Sketchbook of Venice [Finberg CCCXV], Venice: Sunset over Santa Maria della Salute and the
62. D32152	Turner, Joseph Mallord William	Venice: Sunset
63. D32185	Turner, Joseph Mallord William	View of Town, with Yellow Sky
64. D32191	Turner, Joseph Mallord William	Sunset on the Sea
65. D32203	Turner, Joseph Mallord William	Orange Sunset
66. D33479	Turner, Joseph Mallord William	Fribourg, Lausanne and Geneva Sketchbook [Finberg CCCXXXII], Geneva, the Jura Mountains and
67. D33484	Turner, Joseph Mallord William	Fribourg, Lausanne and Geneva Sketchbook [Finberg CCCXXXII], Sunset on a Lake
68. D33501	Turner, Joseph Mallord William	Fribourg, Lausanne and Geneva Sketchbook [Finberg CCCXXXII], Sunset, Lake of Lucerne
69. D33504	Turner, Joseph Mallord William	Fribourg, Lausanne and Geneva Sketchbook [Finberg CCCXXXII], Mont Pilatus: Sunset
70. D35260	Turner, Joseph Mallord William	The Whalers Sketchbook [Finberg CCCLIII], Sea Monsters and Vessels at Sunset
71. D35378	Turner, Joseph Mallord William	Ideas of Folkestone Sketchbook [Finberg CCCLVI], Sunset, over the Water
72. D35392	Turner, Joseph Mallord William	Ambleteuse and Wimereux Sketchbook [Finberg CCCLVII], Yellow Sun over Water
73. D35394	Turner, Joseph Mallord William	Ambleteuse and Wimereux Sketchbook [Finberg CCCLVII], Sunset at Ambleteuse
74. D35927	Turner, Joseph Mallord William	A Lurid Sunset
75. D35943	Turner, Joseph Mallord William	Sunset over Yellow-Green Waters
76. D35950	Turner, Joseph Mallord William	Yellow Sunset
77. D35973	Turner, Joseph Mallord William	The Bass Rock
78. D35986	Turner, Joseph Mallord William	Sunset: Study for "Flint Castle, on the Welsh Coast"
79. D36060	Turner, Joseph Mallord William	The Rigi
80. D36078	Turner, Joseph Mallord William	Sunset. (?Sunrise)
81. D36123	Turner, Joseph Mallord William	The Red Rigi: Sample Study
82. D36149	Turner, Joseph Mallord William	Sunset, with Smoke from a Distant Steamer
83. D36153	Turner, Joseph Mallord William	Distant View of Regensburg from the Dreifaltigkeitsberg
84. D36159	Turner, Joseph Mallord William	Sunset: A Fish Market on the Beach
85. D36174	Turner, Joseph Mallord William	The Walhalla, near Regensburg on the Danube
86. D36211	Turner, Joseph Mallord William	Lausanne: Sunset
87. D36242	Turner, Joseph Mallord William	Geneva
88. D36293	Turner, Joseph Mallord William	Yellow and Blue Sunset over Water
89. D36679	Turner, Joseph Mallord William	Sunset Seen from a Beach with Breakwater
90. N00304	Wilson, Richard	Lake Avernus and the Island of Capri
91. N00309	Gainsborough, Thomas	Boy Driving Cows near a Pool
92. N00342	Callcott, Sir Augus Wall	Dutch Landscape with Cattle
93. N00499	Turner, Joseph Mallord William	The Decline of the Carthaginian Empire...
94. N00519	Turner, Joseph Mallord William	Regulus
95. N00559	Turner, Joseph Mallord William	Petworth Park: Tillington Church in the Distance
96. N00560	Turner, Joseph Mallord William	Chichester Canal
97. N00886	Reynolds, Sir Joshua	Admiral Viscount Keppel
98. N00926	Crome, John	A Windmill near Norwich
99. N01290	Wilson, Richard	Landscape with Bathers, Cattle and Ruin

Atmospheric
aerosols and R/G
ratios in paintings

C. S. Zerefos et al.

Title Page

Abstract Introduction

Conclusions References

Tables Figures

◀ ▶

◀ ▶

Back Close

Full Screen / Esc

Printer-friendly Version

Interactive Discussion



Atmospheric aerosols and R/G ratios in paintings

C. S. Zerefos et al.

Title Page

Abstract

Introduction

Conclusions

References

Tables

Figures

◀

▶

◀

▶

Back

Close

Full Screen / Esc

Printer-friendly Version

Interactive Discussion

Table A1. Continued.

Image ID	Artist Name	Title
100. N01656	McLachlan, Thomas Hope	Evening Quiet
101. N01876	Turner, Joseph Mallord William	Sunset
102. N01902	Brett, John	The British Channel Seen from the Dorsetshire Cliffs
103. N02064	Turner, Joseph Mallord William	The Chain Pier, Brighton
104. N02065	Turner, Joseph Mallord William	A Ship Aground
105. N02066	Turner, Joseph Mallord William	The Arch of Constantine, Rome
106. N02067	Turner, Joseph Mallord William	Tivoli: Tobias and the Angel
107. N02645	Crome, John	Moonrise on the Yare (?)
108. N02647	Wilson, Richard	River View, on the Arno (?)
109. N02701	Turner, Joseph Mallord William	The Lake, Petworth, Sunset
110. N02990	Turner, Joseph Mallord William	Ariccia (?): Sunset
111. N03026	Turner, Joseph Mallord William	Classical Harbour Scene
112. N03382	Turner, Joseph Mallord William	Claudian Harbour Scene
113. N04665	Turner, Joseph Mallord William	Sun Setting over a Lake
114. N04937	Ward, James	L'Amour de Cheval
115. N05361	Crome, John	Yarmouth Harbour – Evening
116. N05486	Turner, Joseph Mallord William	Sunset From the Top of the Rigi
117. N05530	Turner, Joseph Mallord William	Seacoast with Ruin, probably the Bay of Baiae
118. N05853	Boitard, Louis Philippe	An Exact Representation of the Game of Cricket
119. T00921	De Louterbourg, Philip James	Travellers Attacked by Banditti
120. T03163	Garstin, Norman	Haycocks and Sun
121. T03543	Anderton, Henry	Mountain Landscape with Dancing Shepherd
122. T03883	Turner, Joseph Mallord William	The Lake, Petworth: Sunset, Fighting Bucks
123. T03884	Turner, Joseph Mallord William	The Lake, Petworth: Sunset, a Stag Drinking
124. T03885	Turner, Joseph Mallord William	Chichester Canal

Table A2. Volcanic eruptions in 1500–2000 with volcanic explosivity index (VEI) of 4 or more.

No	Year	Volcano	VEI	Reference
1	1522	? Arenal, Costa Rica (C-14: 1525)	4	[1]
2	1568	? Billy Mitchell (C-14: 1580)	6	[1]
3	1586	Kelut, Java	5?	[1]
4	1595	Raung, Java	5?	[1]
5		Ruiz, Colombia	4	[1]
6	1600	Huynaputina, Peru	6?	[1]
7	? ¹ 1605	Momotombo, Nicaragua	4	[1]
8	1622	? Colima, Mexico	4	[1]
9	C-14: 1630	Raoul Island, Kermadec	4	[1]
10	1641	Parker, Indonesia	6	[1]
11	1660	? Teon, Banda	4?	[1]
12		? Guagua Pichinchia, Ecuador	4	[1]
13	1665	? Long Island, New Guinea (C-14: 1660)	6?	[1]
14	1674	Gamkonora, Indonesia	5?	[1]
15	1680	Tongkoko, Sulawesi	5?	[1]
16	1693	Serua, Banda	4?	[1]
17	?1721	Raoul Island, Kermadec (C-14: 1720)	4	[1]
18		Cerro Bravo, Colombia (T)	4	[1]
19	?1737	Fuego, Guatemala	4?	[1]
20	1744	Cotopaxi, Ecuador	4	[1]
21	1760	Michoacan, Mexico	4	[1]
22		Makian, Indonesia	4?	[1]
23	1783	Lakagigar, Iceland	4	[2]
24	1794	? San Martin, Mexico	4?	[1]
25	?1808	Unknown	?	[1]
26	1813	Soufriere St. Vincent, W-Indies	4	[1]
27		Awu, Indonesia	4?	[1]
28		Suwanose-Jima, Japan	4	[1]
29	1815	Tambora, Indonesia	7	[1, 2]
30	1823	Galunggung, Java	5	[1]
31	1831	Babuyan Claro, Philippines	4?	[1]
32	1835	Coseguina, Nicaragua	5	[1, 2]
33	1861	Makian, Indonesia	4?	[1]
34	1875	Askja, Iceland	5	[2]
35	1880	Fuego, Guatemala	4?	[1]
36	1883	Krakatau, Indonesia	6	[1, 2]
37	1886	Tarawera, New Zealand	5	[2]
38	1890	Colima, Mexico	4	[1]
39	1902	Pelee, W-Indies	4	[1]
40		Soufriere St. Vincent, W-Indies	4	[1]
41	1903	Santa Maria, Guatemala	6	[1, 2]
42	1907	Ksudach, Kamchatka, Russia	5	[2]
43	?1911	Lolobau, SW-Pacific	4	[1]
44		Taal, Philippines	4	[1]
45	1912	Katmai, Alaska	6	[2]
46	1953	Ambrym, Vanuatu	4+	[1]
47		Lamington, New Guinea	4	[1]
48		Bagana, SW-Pacific	4	[1]
49	1963	Agung, Indonesia	4	[1, 2]
50	1968	Fernandina, Galapagos	4	[1]
51	1974	Fuego, Guatemala	4	[1]
52	1980	St. Helens, United States	5	[2]
53	1982	El Chichon, Mexico	5	[1, 2]
54	1991	Pinatubo, Philippines	6	[1, 2]

[1]: after Ammann and Naveau (2003) at ftp://ftp.ncdc.noaa.gov/pub/data/paleo/climate_forcing/volcanic_aerosols/ammann2003_eruptions.pdf
 [2]: Robock (2000)

Atmospheric aerosols and R/G ratios in paintings

C. S. Zerefos et al.

Title Page

Abstract Introduction

Conclusions References

Tables Figures

◀ ▶

◀ ▶

Back Close

Full Screen / Esc

Printer-friendly Version

Interactive Discussion



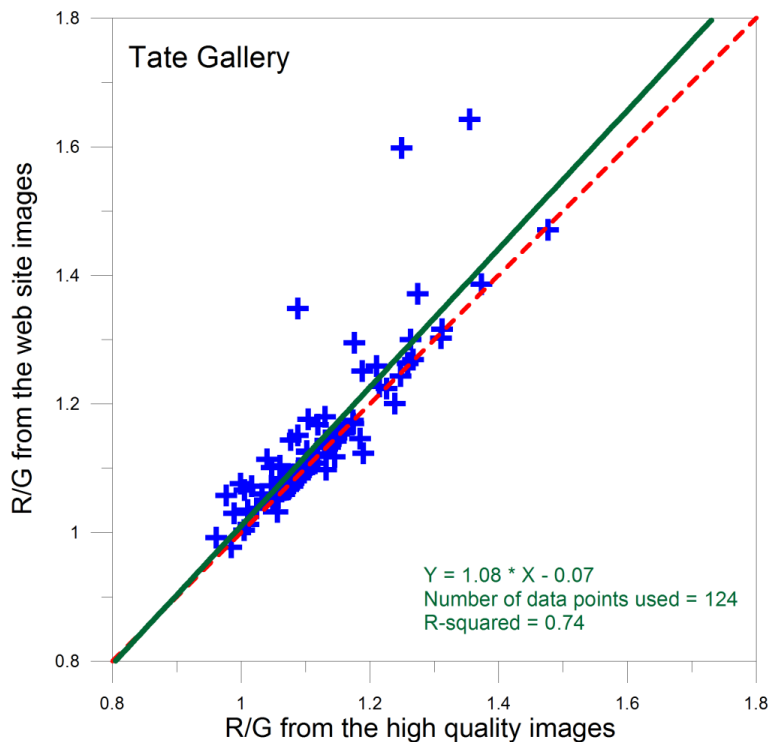


Fig. 1. R/G ratios derived from painting digital images from web site (low resolution) vs. R/G ratios for the same paintings obtained through colour profile protocol (high resolution) at the Tate Gallery. The corresponding linear best fit (green line) and the perfect correlation line (dashed red line) are also shown. The values correspond to the 124 landscape paintings listed in Table A1.

Atmospheric aerosols and R/G ratios in paintings

C. S. Zerefos et al.

Title Page

Abstract

Introduction

Conclusions

References

Tables

Figures

◀

▶

◀

▶

Back

Close

Full Screen / Esc

Printer-friendly Version

Interactive Discussion



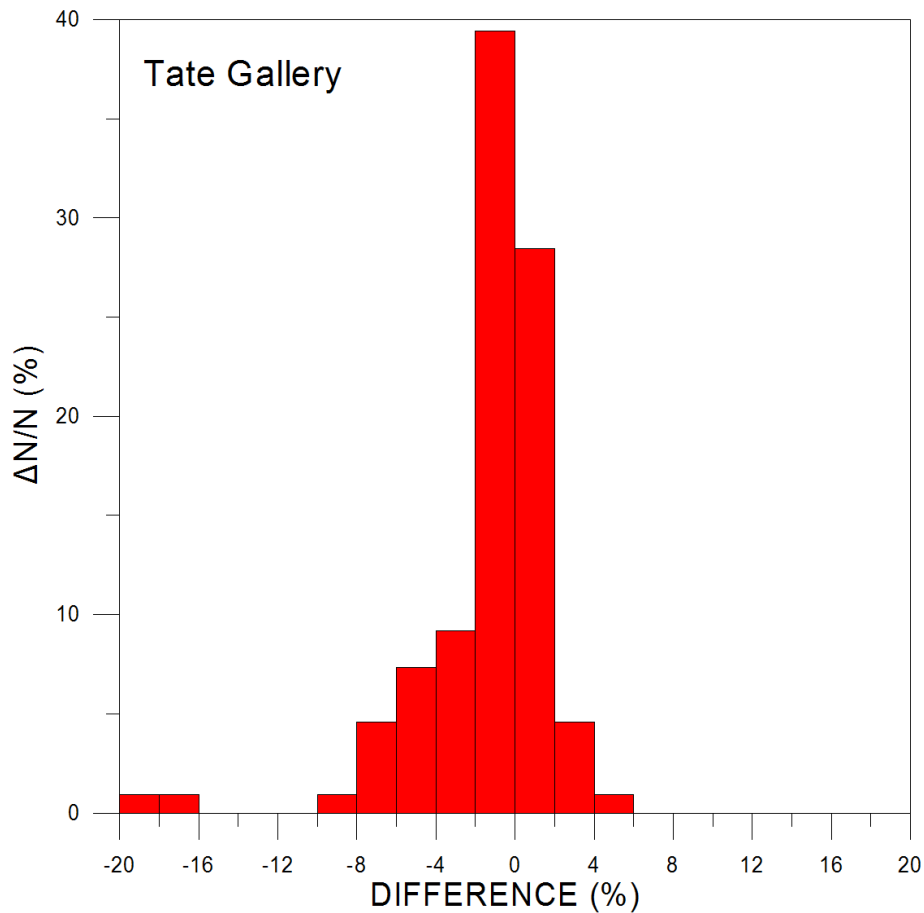


Fig. 2. Distribution of the relative differences (in %) between the RG ratios derived from the high and the low resolution images from 124 landscape sunsets at the Tate Gallery (listed in Table A1).

Title Page

Abstract

Introduction

Conclusions

References

Tables

Figures

◀

▶

◀

▶

Back

Close

Full Screen / Esc

Printer-friendly Version

Interactive Discussion



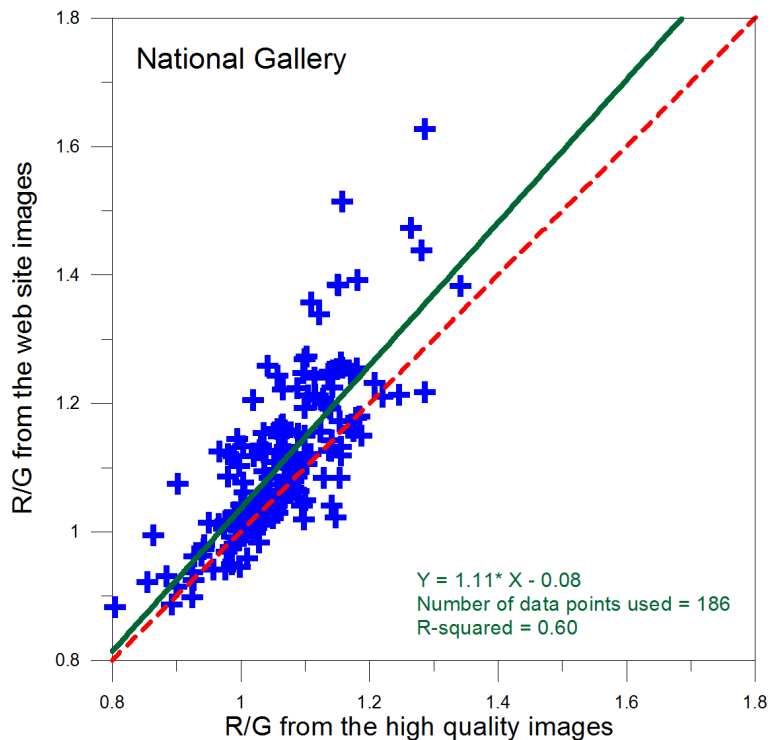


Fig. 3. Results from a completely independent sample of paintings. R/G ratios derived from painting digital images from the web site (low resolution) vs. the same R/G ratios from high resolution digital images at the National Gallery, London. The corresponding linear fit (green line) and the $y = x$ line (dashed red line) are also shown. The values correspond to 186 landscape paintings, which were not used in the early study by Zerefos et al. (2007), as described in the text.

Atmospheric aerosols and R/G ratios in paintings

C. S. Zerefos et al.

Title Page

Abstract Introduction

Conclusions References

Tables Figures

◀ ▶

◀ ▶

Back Close

Full Screen / Esc

Printer-friendly Version

Interactive Discussion



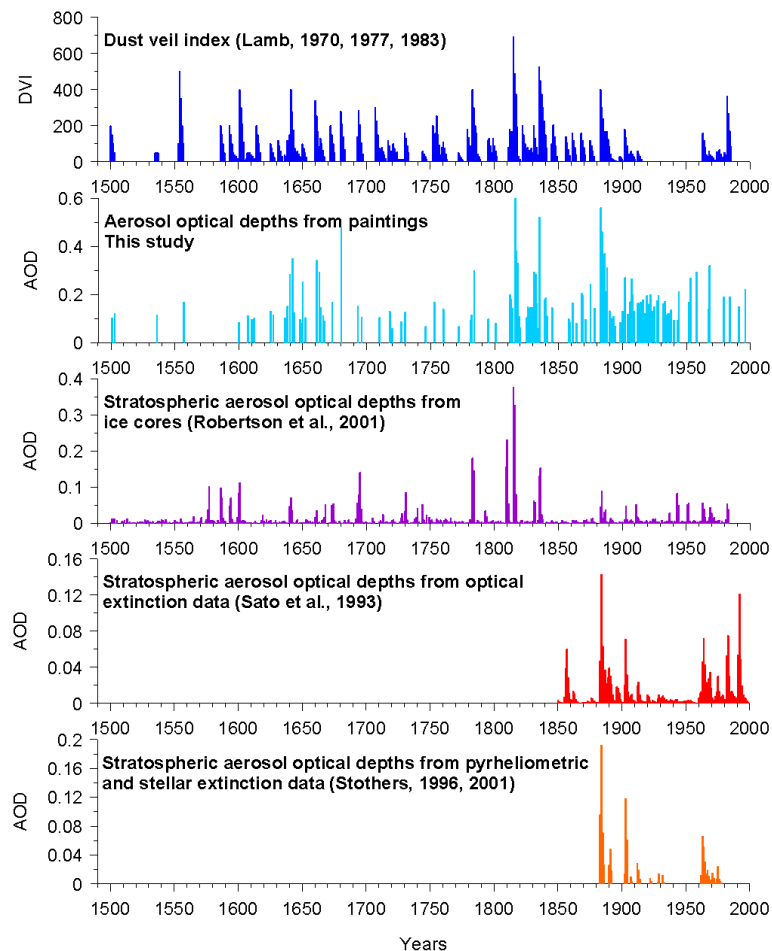


Fig. 4. Aerosol optical depth and other proxy indices during the past 500 yr from different proxies (see text).

Atmospheric aerosols and R/G ratios in paintings

C. S. Zerefos et al.

Title Page

Abstract Introduction

Conclusions References

Tables Figures

◀ ▶

◀ ▶

Back Close

Full Screen / Esc

Printer-friendly Version

Interactive Discussion



Atmospheric aerosols and R/G ratios in paintings

C. S. Zerefos et al.

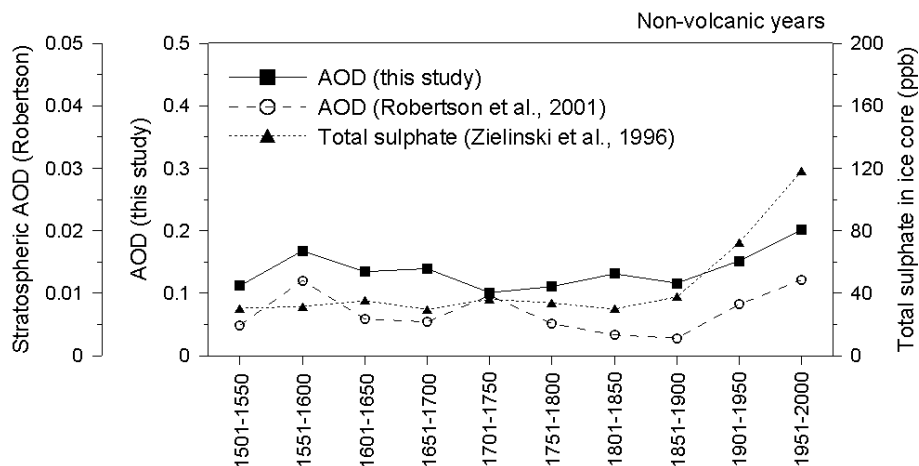


Fig. 5. Total AOD from paintings and in the stratosphere and total sulphate in Greenland ice core (in ppb) averaged over 50 yr intervals for “non-volcanic” years during the period 1500–2000 AD

Title Page

Abstract

Introduction

Conclusions

References

Tables

Figures

◀

▶

◀

▶

Back

Close

Full Screen / Esc

Printer-friendly Version

Interactive Discussion



Atmospheric
aerosols and R/G
ratios in paintings

C. S. Zerefos et al.

Title Page

Abstract

Introduction

Conclusions

References

Tables

Figures

◀

▶

◀

▶

Back

Close

Full Screen / Esc

Printer-friendly Version

Interactive Discussion

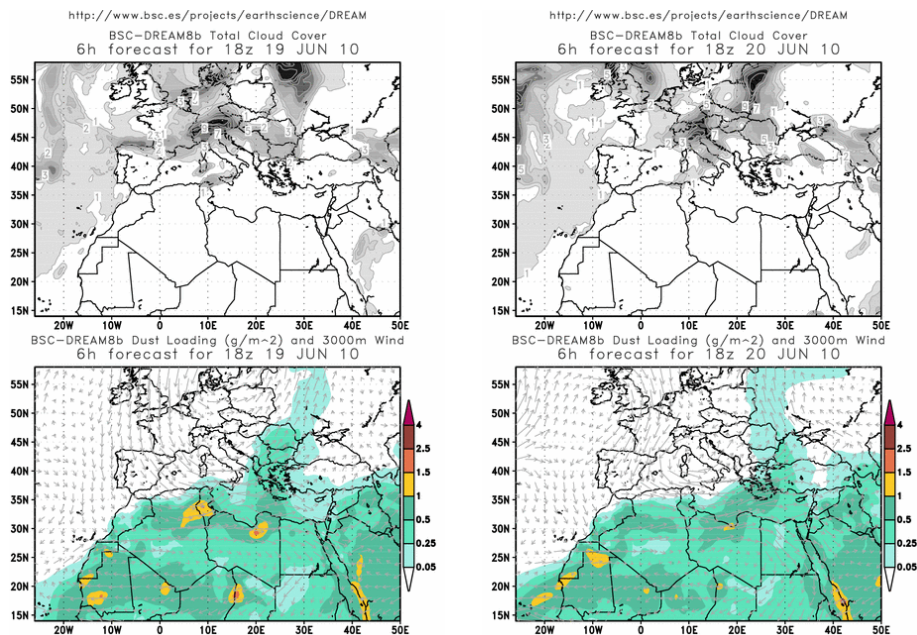


Fig. 6. Dust loading (g/m^2) and 3000 m wind fields over Greece for the 19 and 20 June 2010, as simulated by the BSC/DREAM model (18:00 UTC)

Atmospheric
aerosols and R/G
ratios in paintings

C. S. Zerefos et al.

Title Page

Abstract

Introduction

Conclusions

References

Tables

Figures

◀

▶

◀

▶

Back

Close

Full Screen / Esc

Printer-friendly Version

Interactive Discussion

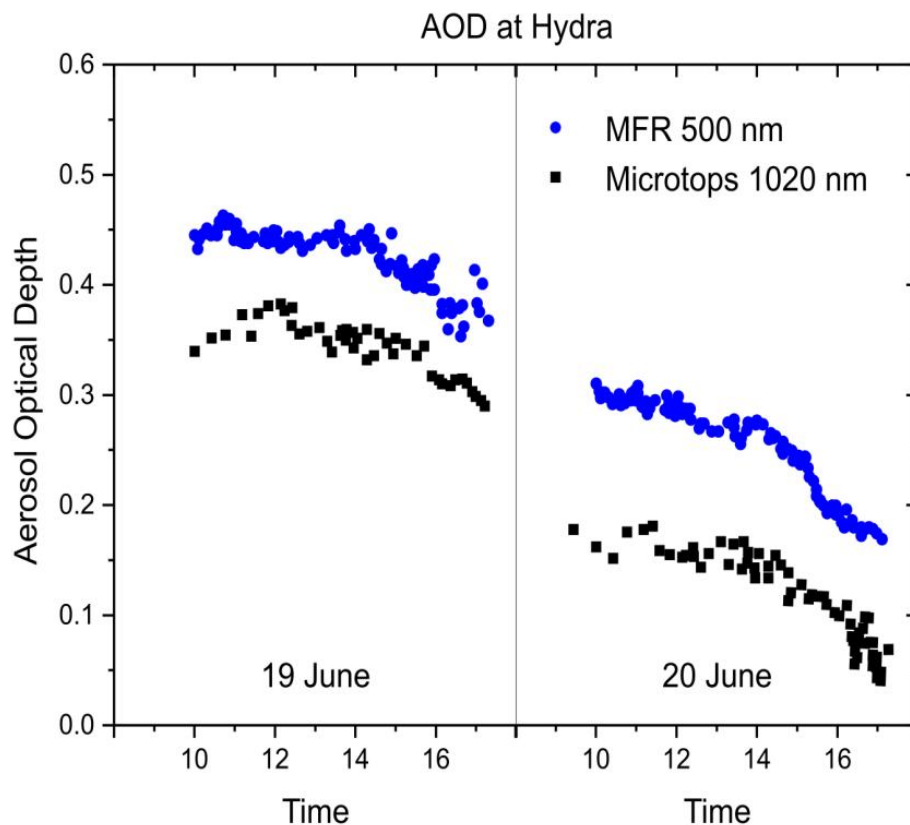


Fig. 7. MFR-7 AOD retrievals at 500 nm on 19 and 20 June 2010 at Hydra campaign site. Microtops II AOD retrievals at 1020 nm are superimposed.

Atmospheric
aerosols and R/G
ratios in paintings

C. S. Zerefos et al.

Title Page

Abstract

Introduction

Conclusions

References

Tables

Figures

◀

▶

◀

▶

Back

Close

Full Screen / Esc

Printer-friendly Version

Interactive Discussion

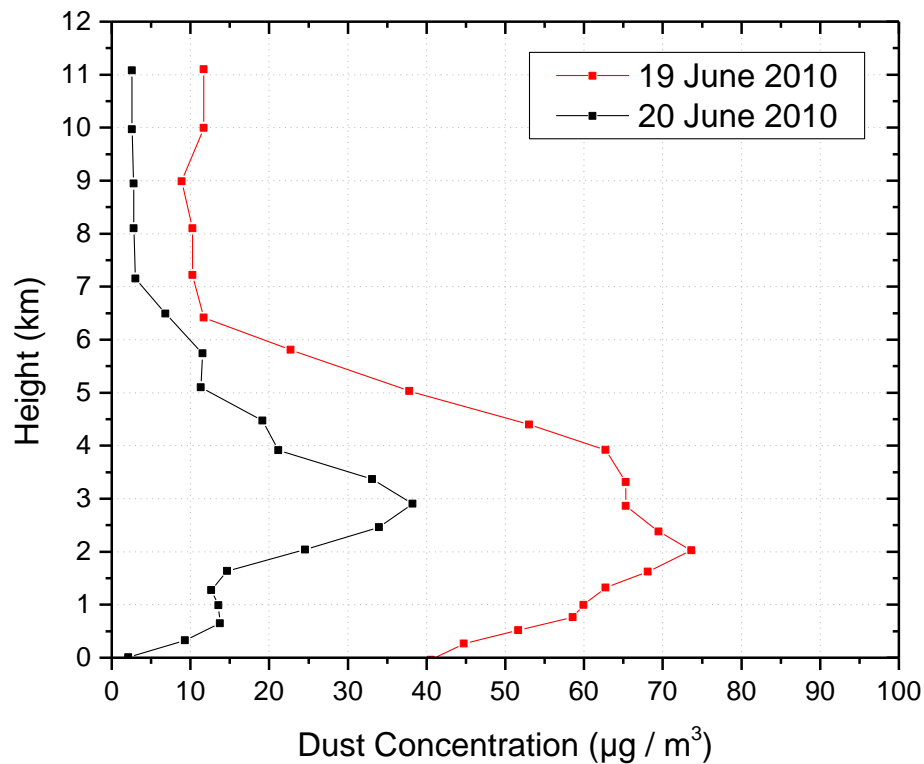


Fig. 8. Vertical distribution of Saharan dust concentration loading ($\mu\text{g m}^{-3}$) for the 19 and 20 June 2010, as simulated by the BSC/DREAM model (18:00 UTC)



Fig. 10. Digitally compressed paintings by P. Tetsis at the Hydra experiment under higher (left panel) and lower (right panel) AOD conditions (see text).